SPECIAL SECTION ON URBAN COMPUTING & WELL-BEING IN SMART CITIES:
SERVICES, APPLICATIONS, POLICYMAKING CONSIDERATIONS

IEEE Access
Multidisciplinary | Rapid Review | Open Access Journal

Received May 22, 2019, accepted June 13, 2019, date of publication June 17, 2019, date of current version July 1, 2019.

Digital Object Identifier 10.1109/ACCESS.2019.2923421

LiDAR-Enhanced Connected Infrastructures Sensing and Broadcasting High-Resolution Traffic Information Serving Smart Cities

BIN LV[1], HAO XU[2], JIANQING WU[2], YUAN TIAN[2], YONGSHENG ZHANG[2], YICHEN ZHENG[2], CHANGWEI YUAN[3], AND SHENG TIAN[4]

[1]School of Traffic and Transportation, Lanzhou Jiaotong University, Lanzhou 730070, China
[2]Department of Civil and Environmental Engineering, University of Nevada, Reno, NV 89557, USA
[3]School of Economics and Management, Chang'An University, Xi'an 710064, China
[4]School of Civil Engineering and Transportation, South China University of Technology, Guangzhou 510640, China

Corresponding authors: Bin Lv (jdlbxx@mail.lzjtu.cn) and Jianqing Wu (jianqingwu2015@gmail.com)

The work was supported in part by the Natural Science Foundation of China under Grant 61463026 and Grant 61463027, in part by the Fundamental Research Funds for the Central Universities under Grant 300102238614, and in part by The Ministry of Education of Humanities and Social Science Project under Grant 18YJAZH120.

ABSTRACT Connected-vehicle system is an important component of smart cities. The complete benefits of connected-vehicle technologies need the real-time information of all vehicles and other road users. However, the existing connected-vehicle deployments obtain the real-time status of connected vehicles, but without knowing the unconnected traffic since there are still many unconnected vehicles and pedestrians on the roads. Therefore, it is urgent to find an approach to collect the high-resolution real-time status of unconnected road users. When it is difficult for all vehicles, pedestrians, and bicyclists to broadcast their real-time status in the near future, enhancing the traffic infrastructures to actively sense and broadcast each road user's status is an intuitive solution to fill the data gap. This paper introduces a new-generation LiDAR-enhanced connected infrastructures that can actively sense the high-resolution status of surrounding traffic participants with roadside LiDAR sensors and broadcast connected-vehicle messages through DSRC roadside units. The system architecture, the LiDAR data processing procedure, the data communication, and the first pilot implementation at an intersection in Reno, Nevada are included in this paper. This research is the start of the new-generation connected infrastructures serving connected/autonomous vehicles with the roadside LiDAR sensors. It will accelerate the deployment of the connected network for the smart cities to improve traffic safety, mobility, and fuel efficiency.

INDEX TERMS Connected-vehicle, LiDAR data, communication platform, smart cities.

I. INTRODUCTION

Connected-Vehicle (CV) technologies have been an important component for the future intelligent transportation system (ITS) and the smart cities [1]. In an ideal CV network, all road users can communicate with each other through wireless communication technologies [2], [3]. The CV technologies have a bunch of benefits, including reducing congestions, improving traffic safety, reducing fuel consumptions, and improving mobility [4]. However, the premise of achieving the complete benefits relies on the shared real-time traffic information of all road users [5]. The current CV deployments could not really provide the expected advantages of the CV network since there are still a large number of unconnected vehicles and pedestrians on the roads [6]. How to find an approach to sensing the high-resolution real-time status of unconnected road users during the transition from the traditional traffic to the full autonomous/connected traffic remains a challenge for traffic engineers and researchers [7]. The roadside infrastructure provides a bridge to build the communication between the unconnected road users and connected vehicles on the road. The vehicle-to-infrastructure communication is a major component of the CV system [8]. In the existing deployment

The associate editor coordinating the review of this manuscript and approving it for publication was Miltiadis Lytras.

pilots, road infrastructures equipped with dedicated-short-range-communication (DSRC) roadside units can broadcast the real-time information to connected vehicles [9], [10]. The information broadcasted by the infrastructures include position correction messages, local map messages, basic safety messages (BSMs)/approaching vehicle aggregators, traffic & rail signal messages (such as Signal Phase & Timing – SPaT), and local weather & road surface messages. When most of the infrastructure information is from the traffic signal controllers and the traffic management center, the BSMs and approaching vehicle warning rely on the received connected-vehicle status. When it is difficult for all vehicles and pedestrians to broadcast their real-time status in the near future, enhancing the traffic infrastructures to actively sense and broadcast each road user's status is an intuitive solution to fill the data gap [11]–[13].

There are already many existing traffic sensors installed along the road network, but data from these conventional traffic sensors are not the high-resolution micro traffic data (HRMTD-mainly including speed, location, direction, and timestamp) required by the CV network. The traditional traffic sensors such as loop detectors, video detectors, Bluetooth sensors and radar sensors mainly provide macro traffic data such as traffic flow rates, average speeds, and occupancy, so the existing sensors cannot offer HRMTD. For example, the conventional video sensors measure vehicle speed using the predefined detection zones, which is actually average speed in the predefined detection zones [14]. HRMTD can be collected by probe vehicles or connected vehicles with the GPS logging function. However, probe vehicles or the low number of connected vehicles provide only sample data of the traffic fleet on roads, while the connected vehicle applications need the data of all road users. Even the latest crowdsourced data, such as real-time travel time information from Wave, is still the macro-level traffic information that is generated by aggregating probe vehicle data. The new sensor technologies need to be explored to enhance the connected traffic infrastructures to sense the HRMTD of all traffic participants.

The Light Detection and Ranging (LiDAR) technology has the capability to detect the surrounding objects with high accuracy and long measuring distance. During each scan, the LiDAR sensor collects a cloud of points with X, Y and Z coordinates of surrounding objects with relatively high accuracy. LiDAR sensors can continuously work without the influence of light conditions. By now, LiDAR sensors are rarely used for roadside deployment because of the historical high price of LiDAR sensors. Fortunately, cost-efficient LiDAR sensors have been manufactured and available on the market [15]. The reduced price allows the deployment of LiDAR sensors along a road network to provide HRMTD of all traffic, which will significantly change the current connected vehicle deployment and other traffic engineering practices. With the new cost-efficient LiDAR sensors, the authors have designed and developed new-generation connected infrastructures that actively sense the high-resolution status of surrounding traffic participants with roadside LiDAR sensors and broadcast connected-vehicle messages through DSRC roadside units. A diagram to demonstrate the principle of the new connected infrastructures is shown in Figure 1.

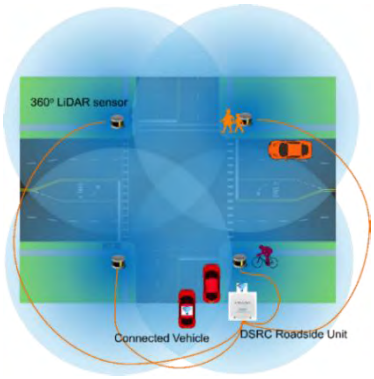

FIGURE 1. Principle of LiDAR-enhanced connected infrastructure sensing and broadcasting HRMTD.

This paper introduces the design of the new connected infrastructures and the first pilot implementation at an intersection in Reno, Nevada. This paper is organized as follows. Section 2 introduces the architecture of the LiDAR enhanced architecture for the hardware components of the system. Section 3 documents the LiDAR data processing flow, which is the key component of the new connected infrastructures. Section 4 is about the data communication system. Section 5 evaluates the performance of the proposed communication system. Section 6 demonstrates the first pilot study of the roadside LiDAR-enhanced infrastructure in the world. The last section summarizes this research and introduces the future effort to extend this study.

II. ARCHITECTURE OF THE LIDAR-ENHANCED CONNECTED INFRASTRUCTURE

The LiDAR-enhanced connected infrastructure integrates roadside LiDAR sensors, connected vehicle technologies, and existing traffic control devices. The system architecture is shown in Figure 2.

A. ROADSIDE SYSTEM

- **Traffic signal controller** – Besides the function of traffic signal control, the traffic signal controller provides the real-time traffic signal information that is packaged as DSRC SPaT messages for broadcasting. It is connected to a field computer through a router with Ethernet cables. The real-time traffic signal information can be read from conventional traffic controllers through the national transportation communications for ITS protocol (NTCIP) [16]. New traffic signal controllers directly provide SPaT messages, such as the Trafficware 980ATC TS-2 Type 2 Signal Controller.
- **Roadside LiDAR sensors** – LiDAR sensors are installed at the four corners (or at two diagonal corners, which is determined by the intersection size and geometry) of an intersection for the full coverage of the

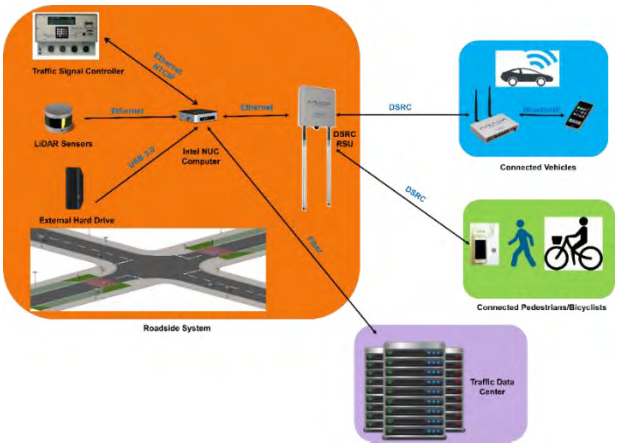

FIGURE 2. System architecture of the LiDAR-based connected infrastructure.

intersection area. For a road segment, the LiDAR sensors are installed along roadsides. The distance between sensors along a road segment is determined by the effective detection range. The 360-degree LiDAR sensors are for real-time detection and tracking of vehicle/pedestrian/bicyclist movement. It needs to be noted that some LiDAR sensors without 360-degree detection angle may also be considered, but this paper focuses on the application of 360-degree LiDAR sensors for its easy installation, maintenance, and data integration. In this research, the roadside LiDAR infrastructure was developed based on the VLP-16 LiDAR sensor. The VLP-16 LiDAR can create 360° 3D point cloud by using 16 laser/detector pairs mounted in a compact housing. The housing rapidly spins to scan the surrounding environment with a range of 100 m (328 ft.). The LiDAR has the rotational speed of 5-20 rotations per second, which can generate 600,000 3D points per second. It can cover 360-degree horizontal field of view (FOV) and a 30-degree vertical FOV. The VLP-16 reports the coordinates in spherical coordinates (r, ω, α), which can be converted into Cartesian coordinates (x, y, z) automatically by the sensor. The roadside LiDAR can be deployed along the roadside permanently. The suitable position for LiDAR installation should consider the detection range (the vertical of the field of view is usually limited) and potential vandalism. The recommended height for the roadside LiDAR deployment is 7ft∼9ft above the ground [17].

- **Field computer** – a field computer at each intersection is to process real-time data from sensors, traffic signal controller and connected vehicles. It packages DSRC messages and communicates with the different roadside components.
- **External hard drives** – external hard drives are optional for field data archiving when the communication from the infrastructure to the data center is not set up or is interrupted.
- **WI-FI router** – a WI-FI router is the hub for the communication of roadside components through Ethernet. It also provides the convenient connection for researchers/engineers to test and debug the system.
- **DSRC roadside unit(s) (RSUs)** – DSRC RSUs are for two-way communication between the connected infrastructure and connected vehicles/pedestrians/bicyclists. It receives the real-time status from the connected vehicles and broadcasts the DSRC messages extracted from the LiDAR data and other data sources.

B. TRAFFIC DATA CENTER

The traffic data center is for the remote traffic operation, data archiving, data integration, traffic performance evaluation, traffic control optimization, traffic data visualization, and other related functions. It is normally connected to the roadside system through the fibers.

C. CONNECTED ROAD USERS

A connected vehicle is equipped with an on-board DSRC communication device and a personal smart device such as smartphones and tablets. The on-board DSRC unit receives real-time DSRC messages. At the same time, the DSRC on-board unit broadcasts its own real-time information to other vehicles and the connected infrastructures. An application on the personal device is connected to the on-board DSRC unit through Bluetooth to receive the real-time traffic data and guide drivers. Connected pedestrians/bicyclists are with portable DSRC units and personal devices such as smart phones. It is a similar system as the connected vehicles.

III. LIDAR DATA PROCESSING

Research efforts have been conducted to process LiDAR data for 3-D feature maps, detecting terrain, vehicles, pedestrians and other objects for robots or autonomous vehicles, which are all for on-board systems [18]. However, the data input and output of on-board sensing systems are different from the extraction of HRMTD from roadside sensors. The LiDAR sensors installed on robots or autonomous vehicles move along with the platforms (robots or vehicles), so the algorithms identify obstacles and other vehicles along the moving path. The roadside LiDAR sensors are fixed and the data processing needs to identify and track the movements of all traffic participants in the detected area. The fixed LiDAR sensors collect data in a larger detection range than the on-board systems with the similar LiDAR sensors, so the roadside LiDAR processing needs to be able to detect and track traffic participants with lower LiDAR point density and lower data quality [19]. When the LiDAR sensors on autonomous vehicles are often merged with vision sensors and radar sensors, the roadside infrastructure needs to rely on the LiDAR sensors only [20]. In this research, combination of LiDAR and video sensors was considered, but this option was suspended with consideration of the expected benefits, the required computational power, and installation/maintenance difficulties. Therefore, a procedure to process roadside LiDAR data is

needed. In the literature review, few existing studies was found to extract HRMTD with roadside LIDAR sensors. The only related research [21] tested the roadside LiDAR to count traffic volumes.

For the specific requirements of the roadside LiDAR data processing, the authors have developed a complete procedure from streaming roadside LiDAR data to the output of HRMTD. The data processing procedure include, background filtering [22], object clustering [23], object classification [24], lane identification [25], and target tracking [10]. The data processing procedure is demonstrated with the flow chart in Figure 3.

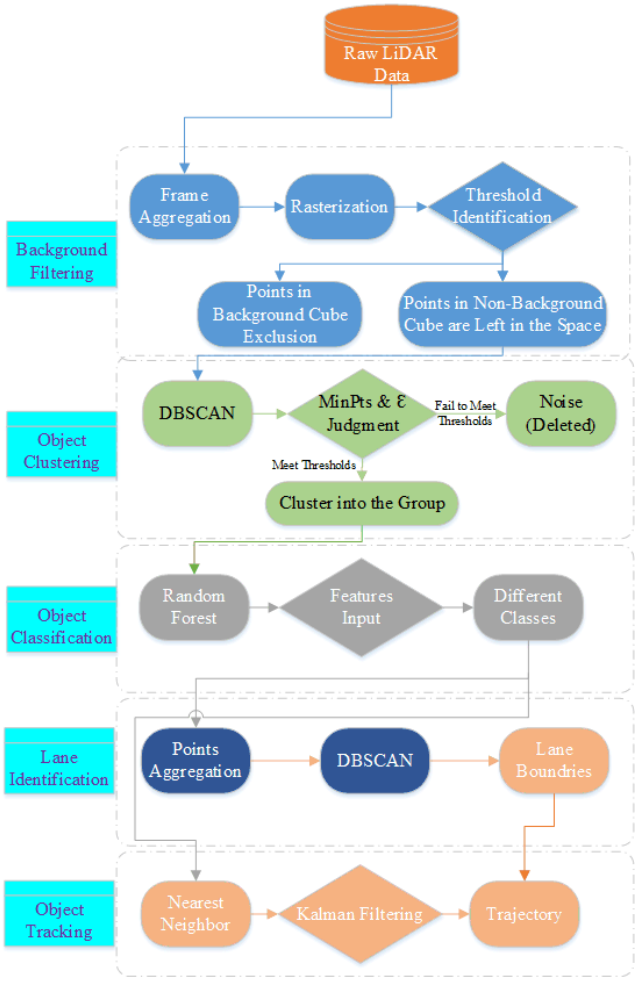

FIGURE 3. LiDAR data processing procedure to extract HRMTD.

A. BACKGROUND FILTERING

The LiDAR creates point clouds for all of its scanned objects, including road users, buildings, trees, and ground surface. The buildings, trees, and ground surfaces were irrelevant information for the HRMTD and were considered as backgrounds. Background filtering is to identify and exclude backgrounds, which is an initial but important step for LiDAR data processing. An automatic background-filtering algorithm was developed in this research to identify and exclude background points from the LiDAR data. The background filtering algorithm includes three major parts: frame aggregation, rasterization, and threshold identification [22]. For one frame, without comparing to other frames, it is difficult to know which cube represents background when there are moving objects in the space. By aggregating multiple frames (1500∼3500) into one coordinate, the density of background points should be higher than that of non-background points. The whole space can be then rasterized into small cubes with the same side length. By giving a pre-defined threshold of point density for each cube, the cube can be identified as background cube or non-background cube [3]. The density threshold for identifying background areas are adaptively adjusted at different distances from the sensor [22]. Then the identified background space is used to exclude the background points from LiDAR data. Any points in the background cubes are excluded from the space. An example of before-after background filtering is shown in Figure 4. The data were collected at the N Virginia St@ 15th St in

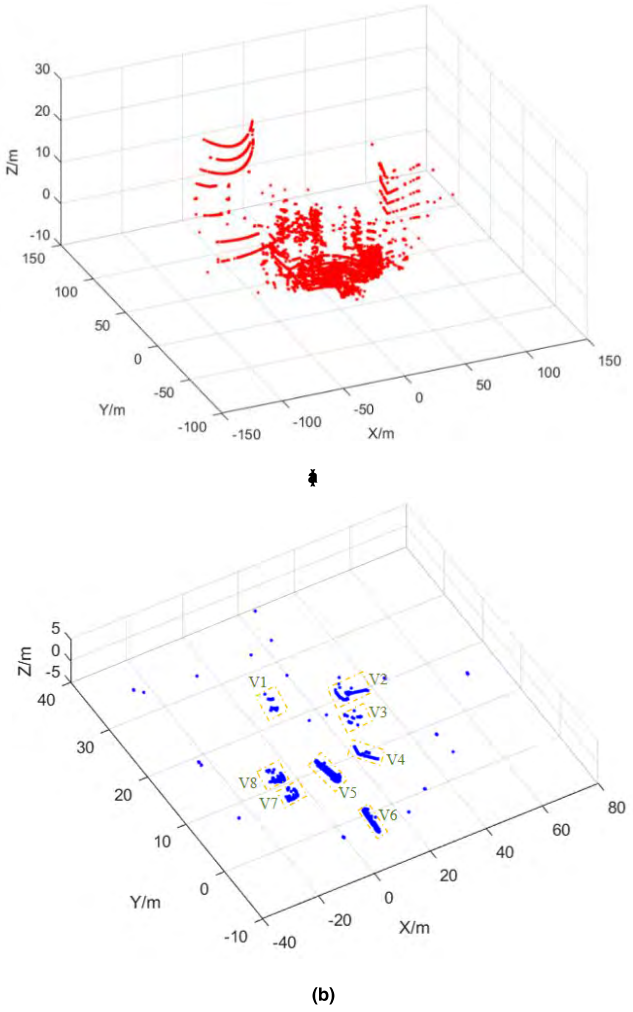

FIGURE 4. Background filtering. (a) Raw LiDAR Points. (b) After Background Filtering.

Reno, Nevada. The LiDAR was permanently installed on the top of the pedestrian signal (about 7ft above the ground). It is shown that most background points were filtered after background filtering.

B. OBJECT CLUSTERING

With the background being filtered and the road/lane boundaries being determined, the LiDAR points in each data frame need to be clustered to identify the traffic participants. The DBSCAN (density-based spatial clustering of applications with noise) [26] method was employed to cluster the LiDAR points. The conventional DBSCAN method was adjusted to adaptively adjust algorithm parameters at the different distances from the LiDAR sensor [14]. The point p whether belongs to one cluster is determined by two parameters: searching radius (ε) and minimal points (MinPts). The ε is used to determine whether another points is the neighborhood (N) of p. The N containing the number of points (nN) equal to or larger than MinPts is considered as high density. Based on ε and MinPts, one point can be assigned to one of the three categories: core point ($p \in N$ & $nN \geq$ MinPts), border point ($p \epsilon N$ & $nN <$ MinPts), and noise point ($p \notin N$). A cluster contains core points and border points. The traditional DBSCAN using the fixed values of ε and MinPts could not cluster the points with varying density. For the points scanned by the roadside LiDAR, the density of points decreased with the increasing distance to LiDAR [27]. Therefore, it is difficult to cluster the points using the fixed MinPts and ε. Dynamic parameters were then developed for DBSCAN considering the LiDAR sensor's mechanical structure and the features of LiDAR points. The primary criterion of ε selection is to make sure points scanned by different beams (different heights) can be detected as the neighbor. Therefore,

$$\varepsilon \geq d \tag{1}$$

where d is the height difference between two adjacent laser beams. d can be estimated based on the distance between point to LiDAR [14], [28]. A recent study [5] showed that the modified DBSCAN can achieve an accuracy of more than 97%.

C. CLASSIFICATION OF TRAFFIC PARTICIPANT TYPES

Type of traffic participants is an important property of the HRMTD for connected vehicles. Distinction between different participant types, mainly pedestrians and vehicles, is needed after the clustering process. The classification of one object is also critical for the analysis of the vehicle-pedestrian conflict [29]. Since the LiDAR can generate the point cloud for its scanned object, the shape information can be generated for each object. The selected features used to distinguish the vehicles and pedestrians include number of points, object length, height profile, difference between height and length, and distance to LiDAR. By comparing the performance of different classification methods including naive Bayes, k-nearest neighbor, support vector machine, random forest, and backpropagation artificial neural network, it was found that random forest can achieve the best performance with the relatively low computing cost [24]. The training results of the random forest model are shown in Table 1.

TABLE 1. Evaluation of the random forest model.

Dataset	Training Set	Validation Set	Testing Set
Total Clusters	600	600	1000
Pedestrians Clusters	413	392	284
Vehicles Clusters	187	208	716
Identified Pedestrians Clusters	407	376	284
Identified Vehicle Clusters	185	205	671
Detection Rate (%)	98.7	96.8	95.5

The data were collected at three sites: Baring Blvd, N Virginia St@15th St, and N Sierra St@11th St in Reno, Nevada. The results showed that 95% and higher accuracy can be obtained with the data collected from different sites.

D. AUTOMATIC IDENTIFICATION OF LANE SPACE

The road/lane location in the 3D space is another important feature for accurate and efficient HRMTD extraction. With the road/lane boundary information, the influence of uninterested objects can be reduced from the data processing. Vehicle/pedestrian tracking can be more accurate in the known road/lane space. This research developed an algorithm to automatically identify boundaries of traffic lanes with aggregated vehicle points. This method firstly aggregates vehicle trajectories in a time period (such as 15 minutes) to learn the vehicle paths, then identifies the road/lane 3D coordinates with the aggregated paths [25]. The vehicle points belonging to the same lane were grouped together using the DBSCAN algorithm. The selected value for ε was 1.2 m and the value for MinPts was 10 based on the regression method developed by Wu *et al.* [3], [25]. This lane identification algorithm can release engineers from the manual lane determination and can avoid any error caused by manual work. Figure 5 shows an example of the lane identification results.

The data were collected at the Baring Blvd at the front of Edward C Reed High School. It is shown that the location of each lane can be generated correctly.

E. OBJECT TRACKING

Tracking is to identify the same object in continuous data frame. The commonly used methods for tracking include nearest neighbor, Kalman Filtering, and multiple hypothesis tracking [30]–[32]. For a vehicle, a single LiDAR sensor can only scan parts of it. A centroid point of the scanned points may change heavily frame by frame. Due to its large size and the tiny time interval between two frames, unstable centroid point will cause extreme systematic bias in speed.

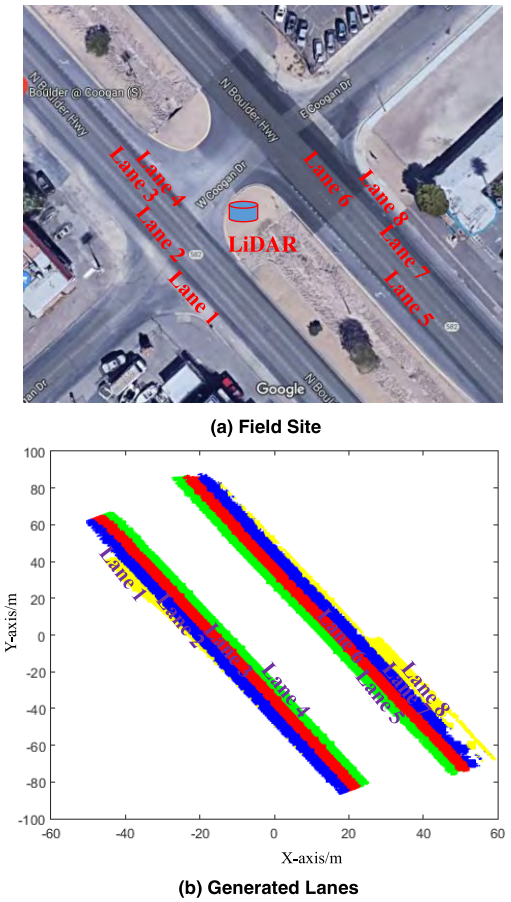

(a) Field Site

(b) Generated Lanes

FIGURE 5. Lane identificatio. (a) Field Site. (b) Generated Lanes.

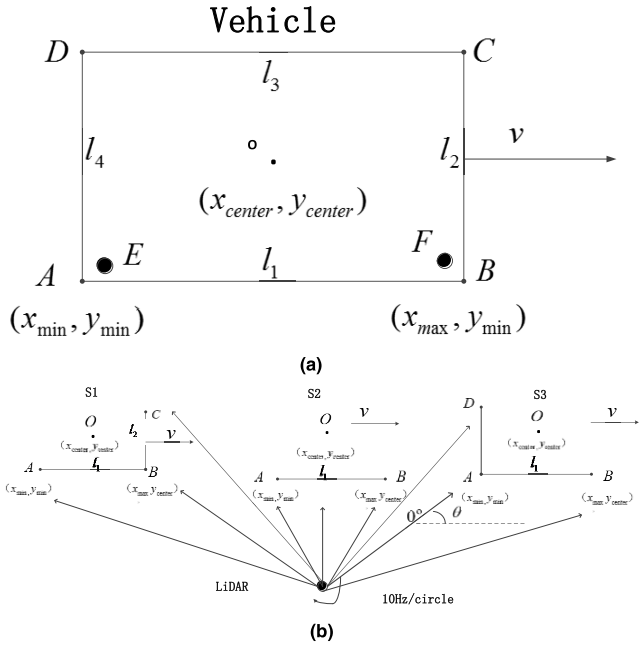

(a)

(b)

FIGURE 6. Different reference points of a vehicle. (a) minimum-area-rectangular calculation. (b) Example of a vehicle at different locations of a LiDAR sensor.

Thus, a corner point with the shortest distance to the sensor is used as the reference point of a vehicle since this point is more stable. The Global Nearest Neighbor (GNN) was applied to track the same vehicles in different frames [33]. Three factors are considered for object tracking – distances between an object in a previous frame to all objects in the current frame, the speed estimated from the historical trajectories, and the time difference between the considered two frames. An object in the current frame is matched to an object in the previous frame, if the distance between the two objects is less than the distance calculated by the estimated speed and time difference. For the case that several objects in the current frame all in the estimated distance range, the object with minimal distance is matched. The tracking uses lane information to limit the searching area. When an object in the current frame cannot find a matched object in the previous frame, a new tracking ID is assigned, which means a new object is detected. For some frames where clusters cannot be detected, the Kalman filter can be used to predict the status of the missing object, thus improving the tracking continuity [14].

F. EXTRACTION OF HRMTD

The major data elements in HRMTD for the connected-vehicle applications include vehicle location, speed, movement direction, and timestamp. When the location, direction and timestamp can be directly obtained from the trajectories. The speed calculation was given a specific consideration. First, the minimum-area-rectangular is calculated for the clustered points of each vehicle, as shown in Figure 6 (a). A, B, C and D points represent the vertices of the rectangular; O is the center point; E and F represent actual vehicle corners estimated with the LiDAR points. E and F points include the timestamp information that is used for speed calculation. The locations of E and F are determined by averaging the LiDAR points in a fixed range of A and B. Vehicle speed can be calculated with the location difference of tracked vehicles in two frames divided by the time difference. Ideally, the corner points E and F, and the center point O can all be used for the calculation. However, when the vehicle is at different locations, the LiDAR points are reflected from different surfaces of a vehicle. A demonstration is shown in Figure 6 (b). When the vehicle is on the left side of the LiDAR sensor, the sensor can detect A, B and C points. When the vehicle is in front of the sensor (the closest location), only A and B points are detected. When the vehicle is on the right side of the sensor, only A, B and D can be detected. That means the corner points closest to the sensor are the most reliable and accurate. So, when the vehicle is approaching the sensor, the front-right corner point F is used for the speed calculation; when the vehicle is leaving the sensor, the rear-right corner point E is used for speed calculation. With data of multiple LiDAR sensors, a vehicle can have more points to describe the shape. In that situation, this developed method still works well to determine the best reference points.

TABLE 2. Data properties included in the HRMTD from roadside LiDAR data.

Property Name	Note
ObjectID	Target ID for tracking an object
ObjectType	Object type. Vehicle, Pedestrian, Bicycle, Wildlife, Obstacle, Other
Date	mm/dd/yyyy
TimeStamp	hh:mm:ss.0
Object_Length	Object length. Feet
Object_Width	Object_width. Feet
TrackPointType	Track point type. CP (center point), FR(front right corner), RR(rear right corner), FL(front left corner), RL(rear left corner)
Coord_x	x value of coordinate of track point (ft)
Coord_y	y value of coordinate of track point (ft)
Coord_z	z value of coordinate of track point (ft)
Coord_dir	direction of polar coordinate degress (0-360) of track point
Coord_dis	distance of polar coordinate of polar coordinate distance (feet) of track point
Longitude	Longitude of track point
Latitude	Latitude of track point
Elevation	Elevation of track point, ft
Direction	Direction of target movement, degree 0-360
Speed	Speed of target movement, MPH

The HRMTD extracted by the data processing includes the properties of each traffic participant, as listed in Table 2. When describing a vehicle's position with X, Y and Z values, the "TrackPointType" tells the reference point of the vehicle coordinate – whether it is the center point or any of the corner points. Table 2 includes more data properties than the DSRC BSM. The content and format of a BSM are defined in Standard SAE J2735. Therefore, the connected vehicle applications can select the needed information from the list. For example, there is no object type element in BSM, so the length value in a BSM can be customized to describe the difference of a pedestrian and a vehicle.

IV. DATA COMMUNICATION

A roadside system named DSRC-Bluetooth communication and mobile application with LiDAR sensor (DBCMA-LS) was developed to stream LiDAR data, package and transfer DSRC basic-safety messages (BSM) via dedicated short-range communications (DSRC). An onboard system was developed to receive, decode the DSRC messages, transfer decoded information through Bluetooth and visualize the LiDAR data in a smart phone application [34].

A. SYSTEM STRUCTURE

The DBCMA-LS system has two major parts: Roadside Unit (RSU) framework and Onboard Unit (OBU) framework, as shown in Figure 7.

The developed DBCMA-LS aims to:

1) Collecting data from different sensors such as connected traffic participants, traffic signals, and roadside LiDAR data.

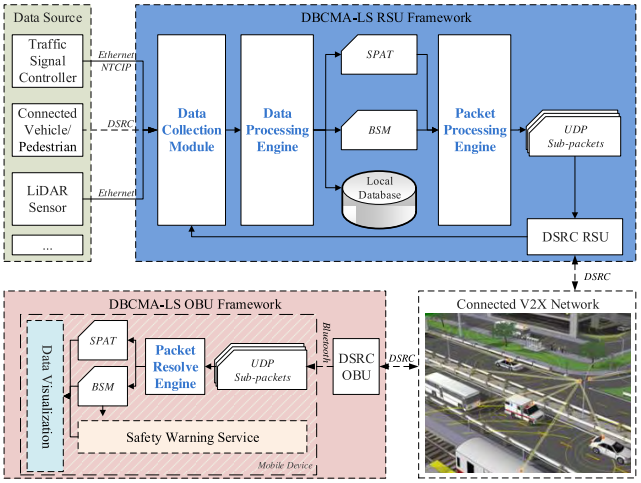

FIGURE 7. DBCMA-LS system structur.

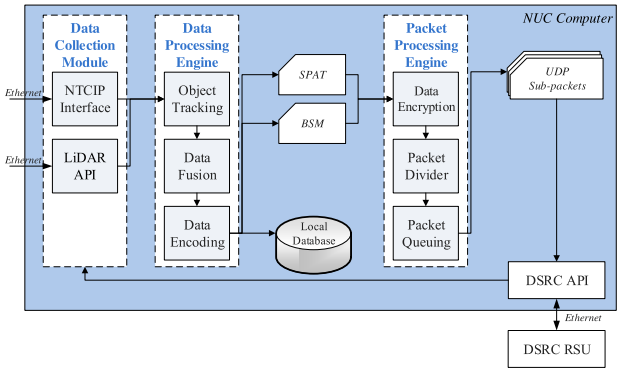

FIGURE 8. Modules in the DBCMA-LS RSU framework.

2) Formatting data into the standard basic safety messages (BSM) and signal phase and timing messages (SPaT).

3) Transferring data from RSU to OBU via DSRC network and from OBU to mobile devices via Bluetooth network.

4) Dividing encoded BSM or SPaT into sub-packets to achieve efficient transmission between on-board DSRC devices and mobile devices through Bluetooth communication.

5) Regrouping and unpacking BSM or SPaT sub-packets in the mobile application.

6) Visualizing the real-time status of other traffic participants and providing a safety alerting service on mobile devices.

B. DBCMA-LS RSU FRAMEWORK

The RSU framework is linked to a commercially available DSRC roadside unit (RSU) that broadcasts and receives DSRC packets. The data collection module, data processing engine, and packet processing engine were implemented in the Next Unit of Computing (NUC) computer [30], as shown in Figure 8.

The data collection module with several standard application-programming interfaces (APIs) was created to

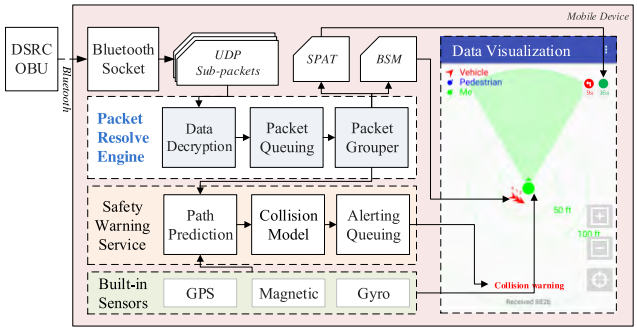

FIGURE 9. Modules of DBCMA-LS OBU framewor.

extract data from different sensors. It can read traffic signal timing data from the traffic signal controller via Ethernet connection based on the National Transportation Communications for ITS Protocol (NTCIP). The data collection module streams roadside LiDAR data via Ethernet based on a custom API.

The data processing engine was used to process the received data and convert them into standard SPaT or BSM messages. The real-time traffic signal timing data is encoded to SPaT messages. The information of road users generated from LiDAR sensor data is integrated in the data fusion module. The combined information of road users is then encoded as BSM messages. The historical data were stored in a local database for debugging.

The encrypted SPaT and BSM messages are to be transferred via DSRC/Bluetooth communication by the user datagram protocol (UDP). A UDP packet needs to go through at least two hops to reach the destination: one hop in the DSRC network and the other hop in the Bluetooth connection. Since the bandwidth decreases and packet loss rate increases in a multi-hop environment, data packets have to be processed in the packet-processing engine to guarantee the communication performance of the system. Data packets are split into smaller sub-packets to meet the bandwidth of the Bluetooth connection.

C. DBCMA-LS OBU FRAMEWORK

The OBU device can receive the real-time SPaT and BSM messages and forward the messages to a mobile device via the Bluetooth connection, as shown in Figure 9. A packet resolving engine implemented in the mobile app regroups the sub-packets, decrypts the data and decodes it to real-time status of road users and traffic signal. The mobile application is used to visualize the received data. The application is also developed to offer the safety warning information to drivers. Connected-vehicle built-in sensors such as GPS/Magnetic/Gyro could be used to help determine the position and direction of the connected vehicle.

Data visualization can help the customers check the real-time traffic situation. A map view is designed to display the user's vehicle and the surrounding road users. The customer can observe the general distance information from displayed distance circles. The zoom and move features of the interface are developed to show traffic participants in the remote area. The real-time traffic signal timing status is displayed at the top-right corner of the screen as a countdown signal head.

In the module of safety warning service, the trajectories of nearby road users can be predicted based on historical speeds, locations, and directions. Then the collision model can evaluate the level of the risk and send a warning message to drivers when the level of the risk is high (by displaying it at the bottom of the screen).

V. ANALYSIS OF DBCMA-LS

A. DELAY AND PACKET-DROPPING PROBABILITY IN THE DSRC/BLUETOOTH NETWORK

The performance of DBCMA-LS relies on the effectiveness and stability of exchanging information between the RSU framework and the OBU framework [35]. The delay and packet-dropping probability of the system are examined to evaluate the performance of DBCMA-LS.

The delay and packet-dropping probability in DSRC network are modeled according to the general scenario - the Institute of Electrical and Electronics Engineers (IEEE) 802.11p-based DSRC communication for a platoon of connected vehicles. In this scene, nodes are all within communication range. As documented in previous studies [36], packet delay can be estimated with

$$D_{DSRC} = \sum_{i=i}^{2n} E\left[D_i\right], \tag{2}$$

where n is the total number of hop; $E[D_i]$ is the average packet delay of hop i, which can be calculated by

$$E[D_i] = E[X_i] \cdot E[s_i], \tag{3}$$

where $E[X_i]$ is the average number of time slots required for successfully transmitting a packet and $E[s_i]$ is the average length of a time slot. In this case, as a general scenario of DSRC communication, $E[X_i]$ and $E[s_i]$ can be treated as constants, and $E[D_i] \approx E[D]$ [36].

The packet-dropping probability is given by

$$p_{DSRC} = 1 - \prod_{i=1}^{2n} (1 - p_{d,i}), \tag{4}$$

where $p_{d,i}$ is the probability that a packet from hop i is dropped. It can also be treated as constant in this case, and $p_{d,i} \approx p_d$.

The typical value of delay $D_{Bluetooth}$ and packet-dropping probability $p_{Bluetooth}$ for the newest version of Bluetooth is applied [33]. The delay and packet-dropping probability are calculated with the assumptions of average packet interval $E[I]$ and average packet size $E[L]$. As a result, all related parameter values are listed in Table 3.

TABLE 3. Parameter values for delay and packet-dropping probability.

Parameter	Description	Values
$E[D]$	Average packet delay in DSRC signal hop	5 (ms)
p_d	Average packet-dropping probability in DSRC signal hop	4.7×10^{-5}
$E[L]$	Average packet size	2048 (byte)
$E[I]$	Average packet interval	200 (ms)
$D_{Bluetooth}$	Average packet delay in Bluetooth connection	20 (ms)
$p_{Bluetooth}$	Average packet-dropping probability in Bluetooth connection	1×10^{-3}

B. SUB-PACKET IN DSRC/BLUETOOTH COMMUNICATION

High-frequency large-size packets produced by the roadside LiDAR data are transferred through the DSRC/Bluetooth network, so they need to be divided into small sub-packets to meet the limitation of both DSRC and Bluetooth connections. When a packet is divided into several sub-packets, the overall delay of the original packet can be shown as:

$$\begin{aligned} D_{nL}(L_S, I) &= (D_{DSRC} + D_{Bluetooth})\left\lceil \frac{L}{L_S} \right\rceil + (\left\lceil \frac{L}{L_S} \right\rceil - 1)I \\ &= (2n \cdot E[D] + D_{Bluetooth})\left\lceil \frac{L}{L_S} \right\rceil + (\left\lceil \frac{L}{L_S} \right\rceil - 1)I \end{aligned} \tag{5}$$

where L is the size of original packet, L_S is the size of the sub-packet, I is the packet interval between sub-packets, and $\lceil\rceil$ is the rounding up operator.

The original packet drops when any of the sub-packets is lost. The packet-dropping probability increases when the packet interval is too small. The packet-dropping probability of the original packet can be described as:

$$\begin{aligned} p_{nL}(L_S) &= 1-[(1-p_{DSRC})(1-p_{Bluetooth})\min(I/E(I), 1)]^{\left\lceil \frac{L}{L_S} \right\rceil} \\ &= 1-\left[(1-p_d)^{2n}(1-p_{Bluetooth})\min(I/E(I), 1)\right]^{\left\lceil \frac{L}{L_S} \right\rceil} \end{aligned} \tag{6}$$

Based on the equations (5) and (6), both delay and packet-dropping probability will increase when a large packet is divided into several sub-packets. L_S and I must be carefully chosen to ensure the performance of DBCMA-LS.

C. PERFORMANCE ANALYSIS OF DBSCMA-LS

In the case of packet loss, an equivalent packet delay is defined to better estimate the actual delay time, shown as

$$\hat{D}_{nL}(L_S, I) = \frac{D_{nL}(L_S, I)}{1 - p_{nL}(L_S)} \tag{7}$$

The DBCMA-LS RSU framework transfers the BSM messages to the mobile application in real time. Therefore, the performance of DBCMA-LS is evaluated according to the average delay of the DBCMA-LS system, which means the equivalent delay of the delivered BSM packet without packet loss, shown as

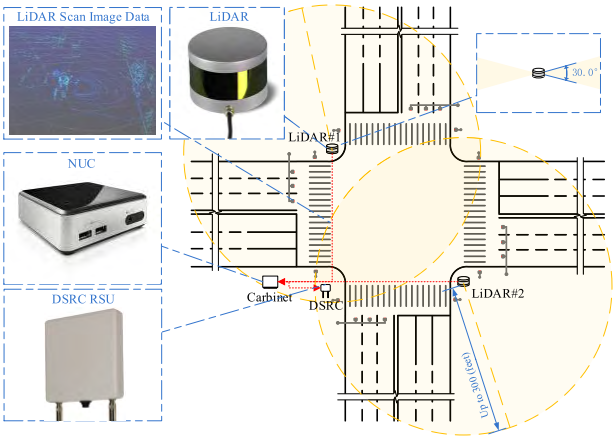

FIGURE 10. Implementation of pilot DBCMA-LS RSU framework.

$$\begin{aligned} D_{DBCMA-LS} &= \frac{1}{n(L_{\max} - L_{\min})} \sum_{n=1}^{n_{\max}} \sum_{L=L_{\min}}^{L_{\max}} \hat{D}_{nL}(L_S, I) \\ &= \frac{1}{n(L_{\max} - L_{\min})} \sum_{n=1}^{n_{\max}} \sum_{L=L_{\min}}^{L_{\max}} \frac{D_{nL}(L_S, I)}{1 - p_{nL}(L_S)} \end{aligned} \tag{8}$$

where $L_{\max}$ and $L_{\min}$ are the maximum and minimum size of the package in the system, and $n_{\max}$ is the maximum size of the DSRC network.

Based on the performance evaluation, the message interval between sub-packets can be chosen to reach the minimum average delay of the DBCMA-LS system. Therefore, the best interval $\hat{I}$ for the packet process engine is calculated by solving the following optimization problem:

$$\begin{aligned} \min_{I} \quad & D_{DBCMA\text{-}LS}(I) = \frac{1}{n\,(L_{\max} - L_{\min})} \\ & \times \sum_{n=1}^{n_{\max}} \sum_{L=L_{\min}}^{I_{\max}} \frac{D_{nL}\,(L_S, I)}{1 - p_{nL}\,(L_S)} \\ s.t. \quad & I \geq I_{\min}, L_{\min} = L_S, L_{\max} = k \cdot L_{\min} \end{aligned} \tag{9}$$

where k is the max number of divided sub-packets, and $I_{\min}$ is the minimum interval required by DSRC/Bluetooth hardware. It should to be noted that $\hat{I}$ varies based on different k and $n_{\max}$; boundary conditions need to be further limited to achieve a global optimal solution.

VI. IMPLEMENTATION OF DBCMA-LS

The world-first DBCMA-LS system with two VLP-16 LiDAR sensors was installed at a signalized intersection around the University of Nevada Reno (UNR), as shown in Figure 10. The field site picture is shown in Figure 11. A microwave antenna was also installed at the intersection and reserved for further wireless communication to the control center at UNR.

FIGURE 11. Field Picture of DBCMA-LS RSU.

The DBCMA-LS OBU system includes the DSRC OBU device and an Android phone with an implemented application, as shown in Figure 12.

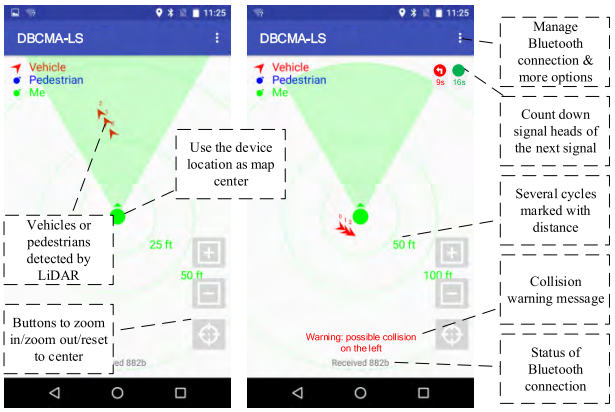

FIGURE 12. DBCMA-LS OBU framework.

OBU device received the traffic information from DSRC and displayed the corresponding information on the map view of the Android application. The map is always centered at the location of the device so that user can monitor the surrounding traffic participants.

The end-to-end packet delay and the packet-dropping probability of the implemented DBCMA-LS system were tested in the field. In the test cases, packets of different sizes (L) were transferred. Different packet intervals (I) of sub-packets were used to seek the optimal communication performance of DBCMA-LS. The interval between two packets was long enough so that packages were not affected by each other. The end-to-end packet delay ($D_{e2e}(L, I)$) was counted by the time difference between the current GPS time on the Android device and GPS timestamp in the BSM message. The end-to-end packet-dropping probability ($p_{e2e}(L, I)$) was calculated by dividing the number of successfully resolved packages by the total number of packages. It was shown in Figure 13 that end-to-end packet delay increased with the increasing packet size. When the packet interval is less than 20 ms, communication becomes congested with the

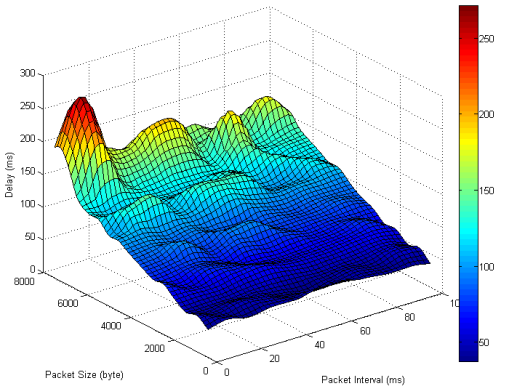

FIGURE 13. End-to-en acket delays.

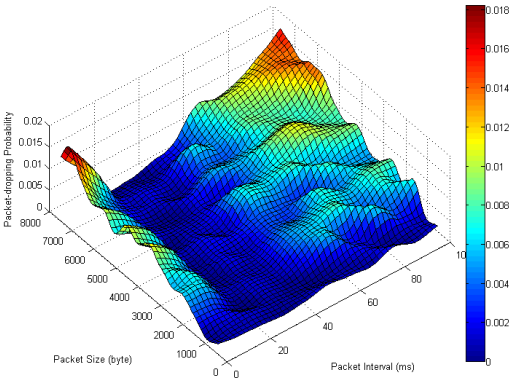

FIGURE 14. End-to-end packet-dropping probabilities.

larger packet size. This can lead to a rapid increase of delay. Figure 14 shows that the packet-dropping probability was relatively low. When the packet interval is less than 20 ms, the packet-dropping probability increases, indicating the reliability of the communication is degraded. With the rise of packet interval and packet size, the sub-packet may be influenced by the following packet. This can increase the packet-dropping probability.

The pilot study shows that when the interval is between 20 and 40 ms, the best performance of the system can be achieved. In this research, $\hat{I} = 30$ ms was selected as the best packet interval. The end-to-end equivalent packet delay ($\hat{D}_{nL}(L_S, \hat{I})\big|_{n=1,Ls=E[L]}$) is shown in Figure 15.

It is shown that the maximum equivalent packet delay was less than 200ms with a packet less than 8 MB. The limited delay can guarantee the real-time applications of the CV network.

VII. SUMMARY

This research is the start of the new-generation connected infrastructures serving connected/autonomous vehicles with

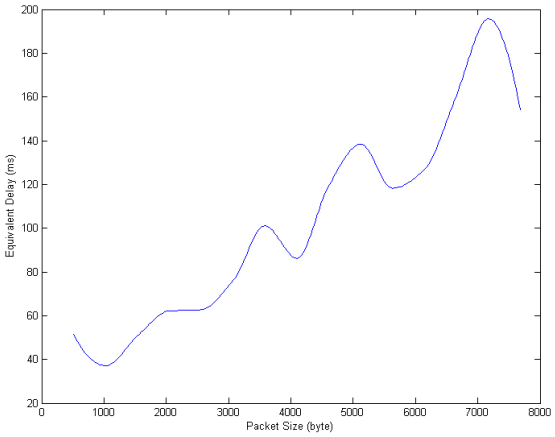

FIGURE 15. Equivalent packet delays of DBCMA-LS.

the roadside LiDAR sensors. The proposed connected-vehicle system is an important component of smart cities. The high-resolution roadside LiDAR data can solve the issue with existing connected vehicle deployments that do not have HRMTD of unconnected vehicles. Full benefits of connected/autonomous vehicles, such as the crash-avoidance applications and Eco-driving applications, can be expected with the new connected infrastructure. The new connected infrastructure can accelerate the deployment of connected-vehicle technologies, and be used as a guidance to deploy LiDAR-based connected infrastructures on other roads, regions and states. This system can collect the HRMTD of unconnected traffic road users and broadcast the HRMTD to the connected vehicles. The drivers can see any possible safety-critical events by receiving the warning information through the developed App. Therefore, the traffic safety can be improved with the proposed system.

Opportunities related to the LiDAR-based connected infrastructure can go beyond connected-vehicle applications. The high-resolution micro traffic data will also change existing traffic safety engineering and traffic operation. For example, the micro-level trajectories of vehicles and pedestrians at intersections can be used to analyze intersection traffic safety and signal performance with much more details than the traditional safety and performance analysis. The existing Rectangular Rapid Flash Beacon (RRFB) for midblock pedestrian crosswalks can be upgraded to an automatic pedestrian signal with the real-time high-resolution micro traffic data. Warning of wildlife crossing highways can be automatically triggered when the real-time micro traffic data shows wildlife crossing. The high-resolution micro traffic data can also support adaptive traffic signal control systems. Unconnected vehicles and pedestrians can all benefit from the high-resolution micro traffic data.

The future research will extend the pilot connected intersection to a segment of the arterial with LiDAR sensors deployed and connected along the road segment. The different intersections and facilities will create different scenarios to demonstrate how the roadside LiDAR data improve safety, mobility and efficiency. The proposed method can help create the connected network for the smart cities. How to integrate the connected-vehicle system with other systems in the smart cities is another research topic. The proposed system may also reduce the fuel consumption of vehicles by providing a better route using the HRMTD data, which can be another important contribution to the smart cities.

REFERENCES

[1] A. Visvizi, M. D. Lytras, E. Damiani, and H. Mathkour, "Policy making for smart cities: Innovation and social inclusive economic growth for sustainability," *J. Sci. Technol. Policy Manage.*, vol. 9, no. 2, pp. 126–133, 2018.

[2] A. Visvizi and M. D. Lytras, "Rescaling and refocusing smart cities research: From mega cities to smart villages," *J. Sci. Technol. Policy Manage.*, vol. 9, no. 2, pp. 134–145, 2018.

[3] J. Wu, H. Xu, and J. Zheng, "Automatic background filtering and lane identification with roadside LiDAR data," in *Proc. IEEE 20th Int. Conf. Intell. Transp. Syst. (ITSC)*, Oct. 2017, pp. 1–6.

[4] J. Wu and H. Xu, "Driver behavior analysis on rural 2-lane, 2-way highways using SHRP 2 NDS data," *Traffic Injury Prevention*, vol. 19, no. 8, pp. 838–843, 2018.

[5] Z. Zhang, J. Zheng, H. Xu, and X. Wang, "Vehicle detection and tracking in complex traffic circumstances with roadside LiDAR," *Transp. Res. Rec.*, to be published.

[6] J. Zheng, S. Yang, X. Wang, X. Xia, Y. Xiao, and T. Li, "A decision tree based road recognition approach using roadside fixed 3D LiDAR sensors," *IEEE Access.*, vol. 7, pp. 53878–53890, 2019. doi: 10.1109/ACCESS.2019.2912581.

[7] B. Lv, H. Xu, J. Wu, Y. Tian, S. Tian, and S. Feng, "Revolution and rotation-based method for roadside LiDAR data integration," *Opt. Laser Technol.*, vol. 119, Nov. 2019, Art. no. 105571. doi: 10.1016/j.optlastec.2019.105571.

[8] J. Wu, "Data processing algorithms and applications of LiDAR-enhanced connected infrastructure sensing," Ph.D. dissertation, Dept. Civil Environ. Eng., Univ. Nevada Reno, Reno, NV, USA, 2018.

[9] J. Zhao, H. Xu, J. Wu, Y. Zheng, and H. Liu, "Trajectory tracking and prediction of pedestrian's crossing intention using roadside LiDAR," *IET Intell. Transp. Syst.*, vol. 13, no. 5, pp. 789–795, May 2019. doi: 10.1049/iet-its.2018.5258.

[10] Y. Sun, H. Xu, J. Wu, J. Zheng, and K. M. Dietrich, "3-D data processing to extract vehicle trajectories from roadside LiDAR data," *Transp. Res. Rec.*, vol. 2672, no. 45, pp. 14–22, Dec. 2018.

[11] M. D. Lytras and A. Visvizi, "Who uses smart city services and what to make of it: Toward interdisciplinary smart cities research," *Sustainability*, vol. 10, no. 6, pp. 1–16, 2018.

[12] E. Uhlemann, "Introducing connected vehicles [connected vehicles]," *IEEE Veh. Technol. Mag.*, vol. 10, no. 1, pp. 23–31, Mar. 2015.

[13] E. Uhlemann, "Connected-vehicles applications are emerging [connected vehicles]," *IEEE Veh. Technol. Mag.*, vol. 11, no. 1, pp. 25–96, Mar. 2016.

[14] J. Zhao, H. Xu, H. Liu, J. Wu, Y. Zheng, and D. Wu, "Detection and tracking of pedestrians and vehicles using roadside LiDAR sensors," *Transp. Res. C, Emerg. Technol.*, vol. 100, pp. 68–87, Mar. 2019.

[15] I. Ashraf, S. Hur, and Y. Park, "An investigation of interpolation techniques to generate 2D intensity image from LiDAR data," *IEEE Access*, vol. 5, pp. 8250–8260, 2017.

[16] J. Zheng, B. Xu, X. Wang, X. Fan, H. Xu, and G. Sun, "A portable roadside vehicle detection system based on multi-sensing fusion," *Int. J. Sensor Netw.*, vol. 29, no. 1, pp. 38–47, 2019.

[17] J. Wu, H. Xu, and W. Liu, "Points registration for roadside LiDAR sensors," *Transp. Res. Rec.*, vol. 2672, no. 45, pp. 14–22, May 2019. doi: 10.1177/0361198119843855.

[18] Z. Y. Zhang, J. Zheng, X. Wang, and X. Fan, "Background filtering and vehicle detection with roadside lidar based on point association," in *Proc. 37th Chin. Control Conf. (CCC)*, Jul. 2018, pp. 7938–7943.

[19] J. Wu, "An automatic procedure for vehicle tracking with a roadside LiDAR sensor," *Inst. Transp. Eng.*, vol. 88, no. 11, pp. 32–37, 2018.

[20] Q. Wang, J. Zheng, H. Xu, B. Xu, and R. Chen, "Roadside magnetic sensor system for vehicle detection in urban environments," *IEEE Trans. Intell. Transp. Syst.*, vol. 19, no. 5, pp. 1365–1374, May 2018.
[21] H. Lee and B. Coifman, "Side-fire lidar-based vehicle classification," *Transp. Res. Rec.*, vol. 2308, no. 1, pp. 173–183, 2012.
[22] J. Wu, H. Xu, Y. Sun, J. Zheng, and R. Yue, "Automatic background filtering method for roadside LiDAR data," *Transp. Res. Rec.*, vol. 2672, no. 45, pp. 106–114, 2018.
[23] Y. He, H. Tan, W. Luo, H. Mao, D. Ma, S. Feng, and J. Fan, "MR-DBSCAN: An efficient parallel density-based clustering algorithm using mapreduce," in *Proc. IEEE 17th Int. Conf. Parallel Distrib. Syst.*, Dec. 2011, pp. 473–480.
[24] J. Wu, H. Xu, Y. Zheng, Y. Zhang, B. Lv, and Z. Tian, "Automatic vehicle classification using roadside LiDAR data," *Transp. Res. Rec.*, to be published. doi: 10.1177/0361198119843857.
[25] J. Wu, H. Xu, and J. Zhao, "Automatic lane identification using the roadside LiDAR sensors," *IEEE Intell. Transp. Syst. Mag.*, to be published. doi: 10.1109/MITS.2018.2876559.
[26] J. Wu, H. Xu, Y. Zheng, and Z. Tian, "A novel method of vehicle-pedestrian near-crash identification with roadside LiDAR data," *Accident Anal. Prevention*, vol. 121, pp. 238–249, Dec. 2018.
[27] J. Zhang, X. Lin, and X. Ning, "SVM-based classification of segmented airborne LiDAR point clouds in urban areas," *Remote Sens.*, vol. 5, no. 8, pp. 3749–3775, 2013.
[28] J. Chen, H. Xu, J. Wu, R. Yue, C. Yuan, and L. Wang, "Deer crossing road detection with roadside LiDAR sensor," *IEEE Aceess*, vol. 7, pp. 65944–65954, 2019. doi: 10.1109/ACCESS.2019.2916718.
[29] J. Wu, H. Xu, Y. Zheng, W. Liu, Y. Sun, R. Yue, and X. Song, "Driver behavior fault analysis on ramp-related crashes/near-crashes using SHRP 2 naturalistic driving study data," in *Proc. 21st Int. Conf. Intell. Transp. Syst. (ITSC)*, Nov. 2018, pp. 2134–2139.
[30] X. Liu, B. Chen, H. Zhao, J. Qin, and J. Cao, "Maximum correntropy Kalman filter with state constraints," *IEEE Access*, vol. 5, pp. 25846–25853, 2017.
[31] Z. Fu, P. Feng, F. Angelini, J. Chambers, and S. M. Naqvi, "Particle PHD filter based multiple human tracking using online group-structured dictionary learning," *IEEE Access*, vol. 6, pp. 14764–14778, Mar. 2018.
[32] Y. Cao, H. Qi, W. Zhou, J. Kato, K. Li, X. Liu, and J. Gui, "Binary hashing for approximate nearest neighbor search on big data: A survey," *IEEE Access*, vol. 6, pp. 2039–2054, 2018.
[33] C. Bo, H. Lu, and D. Wang, "Weighted generalized nearest neighbor for hyperspectral image classification," *IEEE Access*, vol. 5, pp. 1496–1509, 2017.
[34] Y. Zheng, H. Xu, Z. Tian, and J. Wu, "Design and Implementation of the DSRC-bluetooth communication and mobile application with LiDAR sensor," in *Proc. 97th Transp. Res. Board Annu. Meeting*, 2018, pp. 1507–1618.
[35] H. Peng, D. Li, K. Abboud, H. Zhou, H. Zhao, W. Zhuang, and X. Shen, "Performance analysis of IEEE 802.11p DCF for multiplatooning communications with autonomous vehicles," *IEEE Trans. Veh. Technol.*, vol. 66, no. 3, pp. 2485–2498, Mar. 2017.
[36] A. Mourad, S. Muhammad, M. O. Al Kalaa, P. A. Hoeher, and H. Refai, "Bluetooth and IEEE 802.11n system coexistence in the automotive domain," in *Proc. IEEE Conf., Wireless Commun. Netw. Conf. (WCNC)*, Mar. 2017, pp. 1–6.

BIN LV received the B.S. degree in automatic control from Lanzhou Railway Institute, Lanzhou, China, in 1998, the M.S. and Ph.D. degrees in transportation planning and management from Lanzhou Jiaotong University, Lanzhou, in 2003 and 2012, respectively, where he is a Professor. His research interests include traffic signal control, intelligent transportation systems, and traffic big data.

HAO XU received the bachelor's and master's degrees from the Department of Automation, University of Science and Technology of China, in 2004 and 2007, respectively, and the master's and Ph.D. degrees in civil engineering with Texas Tech University, in 2009 and 2010, respectively, where he was a Postdoctoral Research Associate, from 2010 to 2013. Since 2013, he has been an Assistant Professor with the Department of Civil and Environmental Engineering, University of Nevada, Reno. His research focus is in the areas of connected-vehicle applications with roadside LiDAR sensors, driving behavior analysis, traffic safety, and fuel consumption evaluation. He manages the connected-vehicle testing environment with the University of Nevada, Reno. The testing environment promotes interdisciplinary research on connected/autonomous vehicles to improve traffic safety and mobility. His research team has set up a LiDAR-based connected intersection in Reno, Nevada, and is performing research on LiDAR-based connected infrastructures.

JIANQING WU received the B.S. and M.S. degrees in civil engineering from Shandong University, Jinan, China, in 2012 and 2015, respectively, and the Ph.D. degree with the Department of Civil and Environmental Engineering, University of Nevada, Reno, in 2018, where he is a Postdoctoral Research Associate. His research interests include driver behavior analysis, intelligent transportation systems, traffic safety, and big data.

YUAN TIAN received the B.S. and M.S. degrees in control science and engineering from Shandong University, Jinan, China, in 2014 and 2017, respectively. He is currently pursuing the Ph.D degree with the Department of Civil and Environmental Engineering, University of Nevada, Reno, USA. His research interests include intelligent transportation systems and traffic safety.

YONGSHENG ZHANG received the bachelor's degree from the Department of Traffic and Transportation, Hebei Polytechnic University of China, in 2011, and the Ph.D. degree in traffic and transportation planning and management from the Beijing Jiaotong University of China, in 2017. From 2017 to 2018, he was a Postdoctoral Research Associate with the Hong Kong Polytechnic University, Hong Kong. Since 2018, he has been a Postdoctoral Scholar with the University of Nevada, Reno, USA. He is currently working on roadside LiDAR data processing and visualization. His research interests include connected-vehicle applications with roadside LiDAR sensors, individual travel behavior analysis, travel demand prediction, accessibility evaluation and fuel consumption evaluation.

YICHEN ZHENG received the B.S. and Ph.D. degrees from the Department of Automation, Tsinghua University. He is a Research Assistant Professor with the University of Nevada, Reno. His research interests include traffic signal control and simulation, application of LiDAR, and connected-vehicle.

CHANGWEI YUAN received the M.S. and Ph.D. degrees from the School of Economics and Management, Chang'An University. He had been a Postdoctoral Research Associate with Tsinghua University, before his faculty career at Chang'An Univeristy, where he is currently a Professor with the School of Economics and Management. His research interests include traffic planning and operation, industrial economics, and intelligent transporation systems.

SHENG TIAN received the bachelor's degree from the Department of Port Mechanical Engineering, Wuhan University of Technology, in 1991, the master's degree from the Department of Transportation Engineering, Wuhan University of Technology, in 2001, and the Ph.D. degree from the South China University of Technology, where he is an Associate Professor with the Department of Transportation Engineering. He is in charge of over 20 research projects in succession of ''National Natural Science Foundation,'' ''Guangdong Natural Science Foundation,'' ''Science and Technology Plan Projects of Guangdong Province,'' ''Science and Technology Plan Projects of Guangzhou Traffic Committee,'' and ''Science and Technology Projects of Guangdong Province Transportation Department.''